Article

Not peer-reviewed version

VERU-111- Restores Gut Microbial Homeostasis to Promote an Anti-Tumor Response and Facilitate Suppression of Colorectal Cancer

Md Abdullah Al Mamun , Ahmed Rakib , Mousumi Mandal , Wei Li , Duane D Miller , Hao Chen , Mitzi Nagarkatti , Prakash Nagarkatti , Udai P. Singh *

Posted Date: 23 December 2025

doi: 10.20944/preprints202512.1903.v1

Keywords: colorectal cancer; gut microbiota; dysbiosis; metabolic pathways

 doi:10.20944/preprints202512.1903.v1

Article

VERU-111- Restores Gut Microbial Homeostasis to Promote an Anti-Tumor Response and Facilitate Suppression of Colorectal Cancer

Short title: VERU-111 restores healthy gut microbiota

Md Abdullah Al Mamun [1], Ahmed Rakib [1], Mousumi Mandal [1], Wei Li [1], Duane D Miller [1], Hao Chen [1], Mitzi Nagarkatti [2], Prakash Nagarkatti [2] and Udai P. Singh [1]

[1] Department of Pharmaceutical Sciences, College of Pharmacy, 881 Madison Avenue The University of Tennessee Health Science Center, Memphis, TN 38163, USA

[2] Department of Pathology, Microbiology & Immunology, School of Medicine, 6311 G Ferry Road, University of South Carolina, Columbia, SC 29209, USA

* Correspondence: usingh1@uthsc.edu

Abstract

The rising global burden of colorectal cancer (CRC) has now positioned it as the third most common cancer worldwide. Chemotherapy regimens are known to disrupt the composition of the gut microbiota and lead to long-term health consequences for cancer patients. However, the alteration of gut microbiota by specific chemotherapeutic agents has been insufficiently explored until now. The purpose of this study was to assess changes in the gut microbiota following treatment with VERU-111 as a chemotherapy agent for the treatment of CRC. We thus performed a metagenomic study using 16S rRNA gene amplicon sequencing of fecal samples from different experimental groups in the azoxymethane (AOM) and dextran sodium sulfate (DSS)-induced murine model of CRC. To predict the functional potential of microbial communities, we used the resulting 16S rRNA gene sequencing data to perform Kyoto Encyclopedia of Genes and Genomes (KEGG) pathway analysis. We found that the administration of VERU-111 led to a restructured microbial community that was characterized by increased alpha and beta diversity. Compared to the mice treated with DSS alone, VERU-111 treatment significantly increased the relative abundance of several bacterial species, including *Verrucomicrobiota* species, *Muribaculum intestinale*, *Alistipes finegoldii*, *Turicibacter*, and the well-known gut protective bacterial species *Akkermansia muciniphila*. The relative abundance of *Ruminococcus*, which is negatively correlated with immune checkpoint blockade therapy, was diminished following VERU-111 administration. Overall, this metagenomic study suggested that the microbial shift after administration of VERU-111 was associated with suppression of several metabolic and cancer-related pathways that might, at least in part, facilitate the suppression of CRC. These favorable shifts in gut microbiota suggest a novel therapeutic dimension of using VERU-111 to treat CRC and emphasize the need for further mechanistic exploration.

Keywords: colorectal cancer; gut microbiota; dysbiosis; metabolic pathways

1. Introduction

The mammalian intestinal tract is closely packed with its own microbial ecosystem that accommodates over 1,000 operational taxonomic units (OTUs) and more than 40 trillion microorganisms [1,2]. This microbiome serves as a vital regulator that shapes and educates key elements of the host's innate and adaptive immune responses, which in turn regulate and sustain vital aspects of the symbiosis between host and microbes [3]. The microbiome is also deeply involved in regulating other key physiological functions, including vitamin production, altering immune response, pathogen resistance, and nutrient absorption. Consequently, disruptions in the

 doi:10.20944/preprints202512.1903.v1

composition and diversity of the microbiome (known as dysbiosis) are associated with a range of diseases, including cancers [4]. There is also mounting evidence that tumors themselves harbor bacteria and maintain a complex tumor ecosystem [5].

The intestinal microbiome plays a crucial role in both the development of cancer and therapeutic responses to cancer [6]. Mechanistic studies reveal that gut microbiota (GM) can influence the development of colorectal cancer (CRC) by interacting with colonic epithelial cells and host immune response via the production of various metabolites, proteins, and macromolecules [7]. Disruption of this microbial ecosystem can cause a significant threat to the health of the host, leading to the development of not only CRC but also gastrointestinal disorders and neurological, respiratory, metabolic, hepatic, and cardiovascular conditions [8]. Extensive evidence suggests that the GM of CRC patients is distinct from that of healthy individuals and is marked by an increase in harmful taxa and a reduction in protective ones [9]. This altered GM is not only involved in intestinal inflammation and tumor development but also in manipulating the anti-cancer immune response [10].

Disruption of the microbiome compromises the responsiveness of subcutaneous tumors to immunotherapy and platinum-based chemotherapy, while an intact commensal microbiome is required for an optimal response by myeloid-derived cells [11]. Many gut microbial populations, including *Gammaproteobacteria* species, contribute to the development of chemoresistance to gemcitabine therapy in solid tumors [12]. *Fusobacterium nucleatum*, previously recognized for its significant role in tumor initiation and progression, also impacts the risk of CRC, dysplasia, and the outcomes of cancer treatment. Lower levels of *F. nucleatum* are associated with improved prognosis of CRC and higher survival of CRC patients [13,14].

The GM strongly influences the effectiveness of immune checkpoint blockers (ICB) and treatment-associated side effects [15–17]. ICI therapy is a pivotal approach for the treatment of CRC, particularly the CRC subtype associated with deficient mismatch repair, high microsatellite instability (dMMR/MSI-H), and metastatic potential [18,19]. The distinct biological potential of bacteria for improving immunotherapy responses has been explored recently. A synthetic probiotic engineered from *Pediococcus pentosaceus* showed efficacy against CRC with a significant reduction of tumor burden [20]. Also interlinked with CRC growth are GM-derived metabolites, including bile acids, tryptophan metabolites, and short-chain fatty acids are interlinked with CRC growth, which also modulate the immune response [21]. These effects of GM-derived metabolites are context-dependent, and their immunoregulatory functions extend beyond the intestinal compartment to act systemically via both cellular and metabolic pathways [22]. In this study, we used KEGG pathway analysis to obtain a clear picture of changes in metabolic processes after VERU-111 treatment in DSS-induced CRC.

A significant knowledge gap remains in understanding the extent to which chemotherapeutic agents influence the homeostasis of the gut microbiome and alterations in microbiome, in turn, affect the efficacy, toxicity, and overall outcomes of CRC therapies. Addressing this uncertainty and gap is crucial for optimizing treatment strategies and developing novel drug therapies. Our drug candidate VERU-111 is a selective colchicine binding site inhibitor that shows strong antitumor efficacy in multiple solid tumors, including melanoma, breast cancer, lung cancer, pancreatic cancer, and prostate cancer [23–27]. Our previous study revealed the potential of VERU-111 as a treatment for CRC to elicit better outcomes and suppress tumor burden by upregulation of apoptosis, activation of T cells, and downregulation of the programmed cell death protein 1 (PD-1)/ programmed cell death ligand 1 (PD-L1) axis. This study was designed to provide a comparative analysis of the alterations in GM composition following exposure to a carcinogenic agent and subsequent treatment with VERU-111. By examining these microbial shifts, we sought to understand how changes in the GM may influence the therapeutic efficacy of VERU-111 in the context of CRC. Our findings highlight the critical role of GM dynamics in modulating treatment outcomes and underscore the importance of considering microbial factors in the development of effective therapies for CRC and other cancers.

 doi:10.20944/preprints202512.1903.v1

2. Materials and Methods

2.1. Animal Studies

Female 6-8 -week-old C57BL/6 mice were procured from Jackson Laboratories (Bar Harbor, ME, USA). On arrival at our facility, all mice were acclimated for one week under standard housing conditions, including a 12-hour light/dark cycle, in a pathogen-free animal facility at our institution. All experiments were performed under a protocol (number 23–0450) approved by our institution's Institutional Animal Care and Use Committee (IACUC). After the 1-week acclimatization period, mice were randomly divided into control, DSS, and VERU-111-treated experimental groups, each of which contained five mice (n = 5/group). Mice in the control group received normal drinking water throughout the experimental period and received an injection of vehicle alone (PBS) on day 1, while the mice in the DSS and VERU-111 groups received a subcutaneous injection of 10 mg/kg of Azoxymethane (AOM) and were provided with 2.5 % dextran sulfate sodium (DSS) in drinking water from day 3 to day 10, followed by a 10-day recovery period with normal drinking water. This DSS/water cycle was repeated 3 times. Starting from the 7th week, the mice in the treatment group were administered 10 mg/kg VERU-111 via oral gavage 5 days per week for 3 weeks, while mice in the control and DSS groups were administered the vehicle (30% PEG300 in water) orally throughout the treatment period at the same dosing frequency as the VERU-111 group. Body weight and clinical indicators of colitis-associated CRC, including diarrhea, stool consistency, and the presence of blood in feces, were monitored daily until the experimental endpoint.

2.2. Fecal Sample Collection and DNA Isolation

At the endpoint of the experimental protocol at day 60, fecal samples were collected immediately from all mice in 2 mL Eppendorf tubes. All animals were kept in a separate cage to avoid intragroup cross-contamination during the collection of samples. The samples were placed on ice after collection and then stored at -80 °C immediately until further analysis. Frozen aliquots (200 mg) of each fecal sample were thawed, and genomic DNA was extracted using a Qiagen QIAamp DNA Stool Mini Kit (Cat. no. 51604; Qiagen, Valencia, CA) in accordance with the manufacturer's protocol. Immediately upon isolation, the concentration and quality of DNA were determined using a Nanodrop spectrophotometer (Thermo Scientific). Extracted DNA was preserved at -80 °C until further analysis, when it was sent for 16S rRNA sequencing to our collaborator at another institution.

2.3. 16S rRNA Amplicon Sequencing

Total gut microbiota profiling was performed utilizing the 16S rRNA sequencing method on a MiSeq sequencer (Illumina, Illumina Way, San Diego, CA, USA), followed by prediction of potential functional capacities using the Reconstruction of Unobserved States (PiCRUSt) software package. A detailed procedure for 16S rRNA microbial profiling has been described previously [28]. Bacterial DNA libraries of the 16S rRNA V3-V4 hypervariable regions were made by amplification with added Illumina adapter overhang nucleotide sequences prior to sequencing on the Illumina MiSeq platform. The Nephele platform (https://nephele.niaid.nih.gov) from the National Institute of Allergy and Infectious Diseases (NIAID) Office of Cyber Infrastructure and Computational Biology (OCICB; Bethesda, MD) was used to analyze the sequenced reads [29]. Output files were further analyzed with the LefSe Galaxy web application tool developed by the Huttenhower group (Harvard University, Cambridge, MA) to evaluate total gut microbial composition [30]. The PICRUSt2 software package was used to perform KEGG pathway analysis of our 16S rRNA gene amplicon sequencing data at levels 1, 2, and 3 to produce heatmaps that show the predicted changes in GM function for control, DSS, and VERU-111-treated animals.

 doi:10.20944/preprints202512.1903.v1

2.4. Statistical Analysis

All data are presented as mean values ± standard error of the mean (SEM). Statistical analyses were performed using either one-way analysis of variance (ANOVA) followed by Tukey's multiple comparison tests (as indicated in the figure legends) or Student's T-test, depending on the experimental groups, to determine the significance level. A p-value of 0.05 was the level of significance used in all analyses (* $p < 0.05$, ** $p < 0.01$, *** $p < 0.001$, and **** $p < 0.0001$). Graphs were generated using GraphPad Prism software (GraphPad Software, Boston, MA).

3. Results

3.1. VERU-111 Treatment Reversed Overall Gut Microbiota Dysbiosis

Given that the alteration in the composition and function of microbiota contributes to the induction of CRC, we assessed changes in alpha and beta diversity of the gut microbiome under different experimental conditions. We evaluated the modulation that results after treatment of experimental mice with the novel anticancer agent VERU-111 and observed that VERU-111 treatment significantly improved gut microbial alpha diversity, as evidenced by improved Shannon and Simpson indices when compared to DSS alone (**Figure 1A,B**). Next, we analyzed beta diversity across the three experimental groups and performed principal coordinate analysis (PCoA), which revealed a clear separation among the GM of the different experimental groups. Each group was situated in a separate area of the PCoA axis, indicating a change in the overall structure of the GM on induction of CRC with AOM/DSS and treatment with VERU-111. The Bray–Curtis coefficient (PCo) calculates the dissimilarity between the samples based on the abundance of different taxa in each group of samples. We observed a significant difference in the GM composition in the different experimental groups using the Bray–Curtis model (**Figure 1C-F**). Taken together, our data suggests that VERU-111 improves both α- and β-diversity of the GM, underscoring its safety and potential to enhance chemotherapeutic efficacy in the context of CRC.

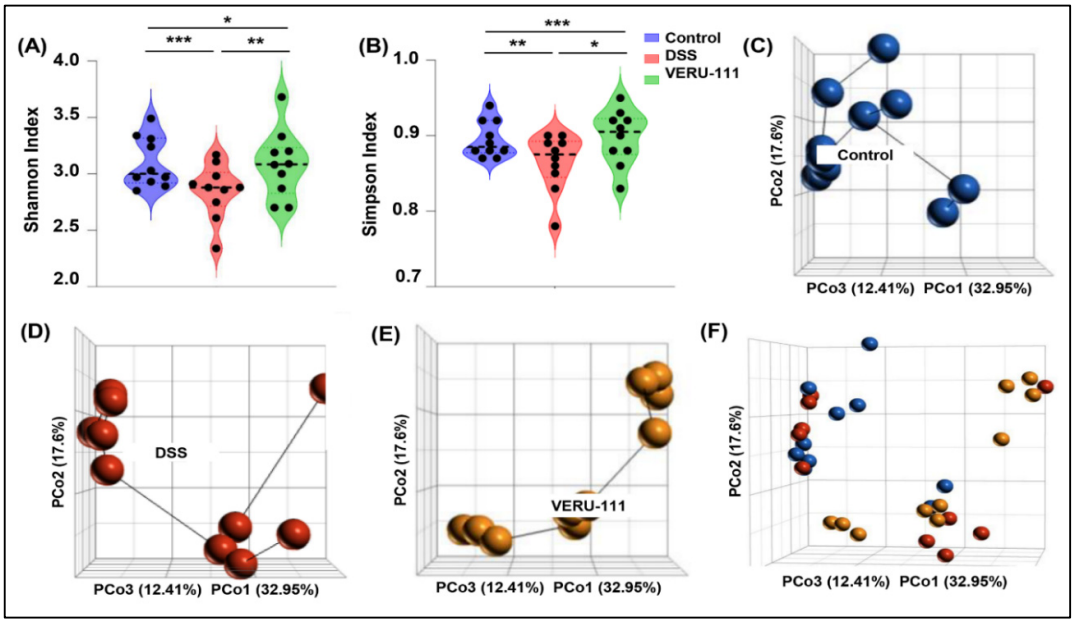

Figure 1. Overall representation of gut microbial diversity alteration in different experimental groups (n=10). Alpha-diversity was analyzed using **(A)** the Shannon index and **(B)** the Simpson index. Violin plots show distribution, with individual samples represented as dots. Principal coordinate analysis (PCoA) was conducted on bacterial beta-diversity based on the Bray–Curtis dissimilarity of gut microbial populations and is represented as three-dimensional PCoA plots of the **(C)** Control, **(D)** DSS, and **(E)** VERU-111 groups. **(F)**

 doi:10.20944/preprints202512.1903.v1

Combined PCoA plot including overlaid PCoA representation of all three groups. Percent variance explained by PCo1, PCo2, and PCo3 is indicated on the corresponding axes. Statistical significance was determined using one-way ANOVA with Tukey's multiple comparison tests (* $p < 0.05$, ** $p < 0.01$, *** $p < 0.001$, and **** $p < 0.0001$).

3.2. VERU-111 Modulated Gut Microbiota and Favored Beneficial Bacterial Phyla

Previous reports describe a notable difference in overall gut microbial composition at the phylum level between healthy individuals and individuals with CRC [31]. Samples from healthy individuals were enriched in *Planctomycetes* species, while samples from individuals with CRC contained elevated levels of *Bacteroides* and *Dorea* species [32]. The potent anticancer and cytotoxic metabolite-producing taxon *Actinobacteria,* plays a pivotal role in influencing tumor suppression [33]. In the current study, a gut microbiota abundance heatmap analysis of samples from mice treated with VERU-111 revealed phylum-level changes in the GM, including a marked increase in beneficial bacterial populations of *Actinobacteria* and *Planctomycetes* after treatment and a noticeable reduction in harmful and CRC-associated taxa *Bacteroidetes* and *Baineolaeota* (**Figure 2A**). Next, we analyzed microbial alterations across taxonomic levels, from phylum to species; the most significantly increased or dysregulated populations are shown (**Figure 2B,C**). Interestingly, treatment with VERU-111 produced a clear restorative effect on DSS-induced dysbiosis, as shown by consistent shifts in microbial composition across both taxonomic analyses. Towards this, we observed a marked increase in *Verrucomicrobiota* that corresponded to a rise in *Akkermansiaceae* at the family level in the VERU-111–treated group compared with the group treated with DSS alone (**Figure 2C**). At the genus and species levels, we observed an increased abundance of *Muribaculum intestinale* bacteria, which are known to be beneficial for CRC outcomes, and a significant reduction in CRC-associated detrimental taxa *Anaeroplasma* (**Figure 2B**). Collectively, these findings suggest that VERU-111 not only mitigates DSS-induced dysbiosis but also fosters a microbiome that is enriched in protective, health-promoting bacterial communities, underscoring its therapeutic potential in shaping gut microbial ecology.

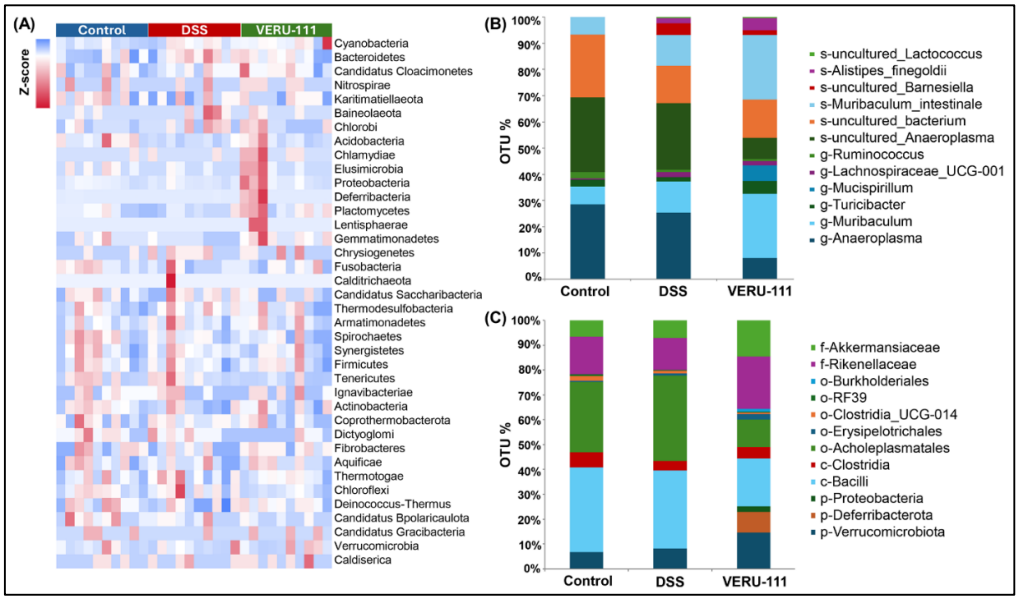

Figure 2. Relative abundance of bacteria at different taxonomical levels in different experimental groups. (A) Heatmap of gut microbiota abundance across three experimental groups. Shown are Z-score–normalized relative abundances of bacterial taxa (n=10). **(B)** Genus and species-level composition analysis. Stacked bar plots depict the relative abundance of dominant genres across groups. **(C)** Phylum to Family level community distribution. Stacked bar plots depict relative abundances at higher taxonomic levels.

 doi:10.20944/preprints202512.1903.v1

3.3. VERU-111 Enhanced the Abundance of Protective Bacteria and Created a Tumor-Suppressing Gut Environment

These promising results led us to conduct a detailed analysis of the relative frequency of each taxon after VERU-111 treatment. The data revealed an increased relative abundance of *Verrucomicrobiota*, a modest reduction in *Proteobacteria*, and no appreciable change in *Deferribacterota* (**Figure 3A-D**). At the class level, we observed no significant change in class *Clostridia*, whereas we observed a notable suppression of Gram-positive class *Bacilli* in the VERU-111-treated group **(Figure 3E-G)**. Given that the functional role of microbes within the class *Bacilli* is multifaceted, with some species reported to confer protective effects and others implicated in CRC progression and adverse outcomes [34,35], we evaluated the changes in the GM at the order and family levels, aiming to make a comprehensive summary of the effects of VERU-111 treatment. We observed a pronounced reduction in bacteria from the order *Acholeplasmatales* (**Figure 4A,B**). To date, there is limited evidence supporting either a positive or a negative role for bacteria from this order in modulating CRC or influencing therapeutic interventions, including immunotherapy. Given the sharp decrease in this population and our findings of tumor suppression after VERU-111 treatment, the shift in the order *Acholeplasmatales* may provide new insights into its potential role in CRC. Consistent with this observation, we observed at the family level a decrease in the abundance of family *Acholeplasmataceae* (order *Acholeplasmatales*) (**Figure 4D**). Overall, we also observed an increase in many healthy GM flora, including members of the *Rikenellaceae* and *Akkermansiaceae*, following treatment with VERU-111 (**Figure 4E,F**). Members of the family *Akkermansiaceae* are well known for their protective role, and *Akkermansia muciniphila* has been reported as a promising immunomodulatory microbiome in the context of CRC. However, the role of bacteria from the *Rikenellaceae* family is still controversial [36]. Taken all together, VERU-111 showed a gut environment enriched in protective bacteria that might serve to suppress tumors, at least in part. However, further detailed investigation will be required to draw a prudent conclusion.

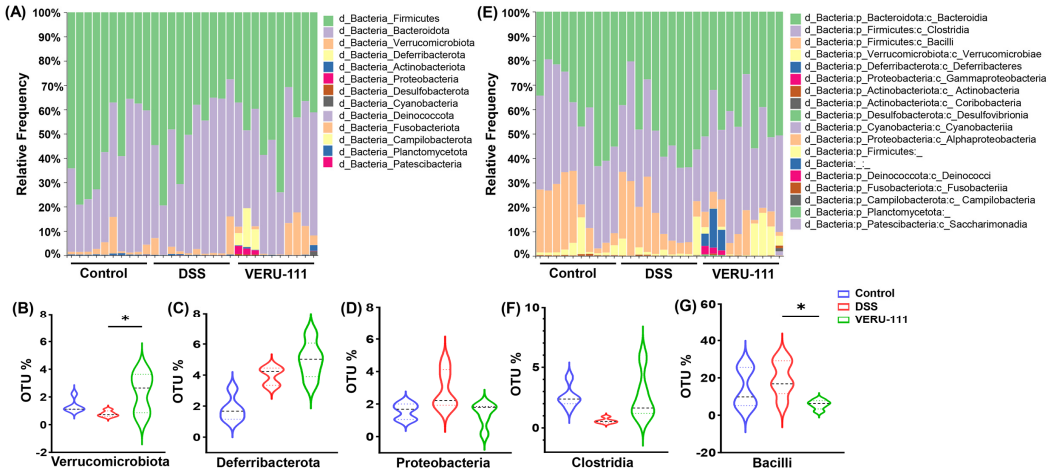

Figure 3. Phylum-level changes of gut microbiota in three experimental conditions. (A) Stacked bar plots of phylum-level microbial community structure depict the relative abundance of major bacterial phyla across the Control, DSS, and VERU-111 groups. DSS exposure shifted the gut microbial composition towards dysbiosis, characterized by a decreased abundance of the Firmicutes and *Verrucomicrobiota* phyla and an expansion of dysbiosis-associated phyla, including *Proteobacteria* and *Deferribacterota*. VERU-111 treatment partially restored microbial balance, increasing beneficial phyla and reducing DSS-induced expansion. **(B–D)** Quantitative comparison of selected phyla. **(B)** Violin plots show a significant increase in *Verrucomicrobiota* after VERU-111 treatment. **(C)** *Deferribacterota* levels trended higher in mice treated with DSS and VERU-111 mice, but the difference was not statistically significant. **(D)** *Proteobacteria* were elevated in mice treated with DSS but reduced after VERU-111 treatment. **(E)** Class-level microbial distribution. Stacked bar plots illustrate the relative abundance of major bacterial classes in three different experimental groups. **(F)** DSS challenge had no notable

 doi:10.20944/preprints202512.1903.v1

effect, while VERU-111 slightly increased the level of *Clostridia*. **(G)** The violin plot represents a significant reduction in the frequency of *Bacilli* upon VERU-111 treatment. Violin plots represent mean ± SEM. Statistical significance was determined using one-way ANOVA followed by Student's t-test (* $p < 0.05$).

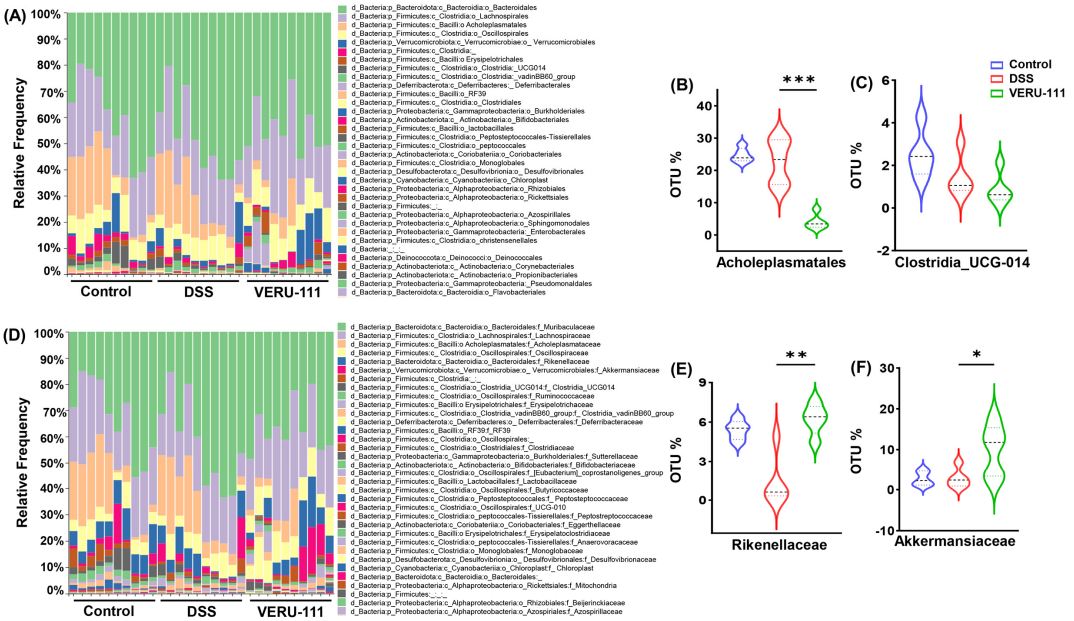

Figure 4. Impact of VERU-111 treatment on gut microbiota composition and alteration of specific bacterial taxa. (A) Stacked bar plots showing the relative abundance of bacterial taxa across three experimental groups at the order level. **(B)** Violin plot showing the percentage of Operational Taxonomic Units (OTUs) for *Acholeplasmatales*. **(C)** *Clostridia_UCG-014* OTU % showed no significant differences among groups. **(D)** Stacked bar plots show the relative abundance of bacterial taxa across three experimental groups at the family level. In the VERU-111-treated mice, violin plots show **(E)** a significant increase of *Rikenellaceae* and **(F)** significantly elevated OTU% for *Akkermansia*. Violin plots represent mean values ± SEM. Statistical analysis was performed using one-way ANOVA followed by Student's t-test. (* $p < 0.05$, ** $p < 0.01$, *** $p < 0.001$).

3.4. VERU-111 Improved the Abundance of Gut-Friendly Bacteria to Increase the Effectiveness of Chemotherapy

We then assessed genus and species richness to identify specific bacteria that are enriched or depleted on VERU-111 treatment. In congruence with our family-level data, we observed a remarkable increase in genus *Akkermansia* and a decrease in genus *Anaeroplasma* on treatment of mice with VERU-111 (**Figure 5A,B**). We also observed a significant increase in genus *Muribaculum* in the VERU-111-treated group relative to that treated with DSS alone (**Figure 5C**). A notable increase in genus *Muribaculum* is positively correlated with CRC, as *Muribaculum* species have the potential to sustain intestinal homeostasis via utilization of mucin-derived monosaccharides [37]. The VERU-111-treated group also exhibited an increase in *Turicibacter* and *Runococcus* but no notable changes in *Lachnospiraceae* relative to the mice treated with DSS alone (**Figure 5C-F**). *Turicibacter* species exert protective effects in the host by stimulating the production of beneficial microbial metabolites, including short-chain fatty acids such as butyrate, and in vitro promote ROS-mediated apoptosis [38].

We observed a significant decrease in the abundance of uncultured *Anaeroplasma* species in the VERU-111-treated group relative to that in the DSS group (**Figure 6A,B**). *Anaeroplasma* is associated with increased inflammation and is present at elevated abundance in samples from patients with untreated CRC [39]. *Muribaculum intestinale* is a healthy GM species that is well recognized for its positive correlation with producing butyrate and reducing cancer cachexia [40]. The abundance of *Alistipes finegoldii* is associated with an improved response to immunotherapy and boosts antitumor

 doi:10.20944/preprints202512.1903.v1

immunity in solid tumors [41]. In this study, we observed a substantial increase in the populations of *Muribaculum intestinale* and *Alistipes finegoldii* at the species level (**Figure 6C,D**). Collectively, these findings suggest that VERU-111–induced alterations in the GM profile are beneficial modulations that boost the pharmacological efficacy of VERU-111 as a chemotherapeutic and provide a foundation for the development of novel microbiota-targeted therapeutic strategies.

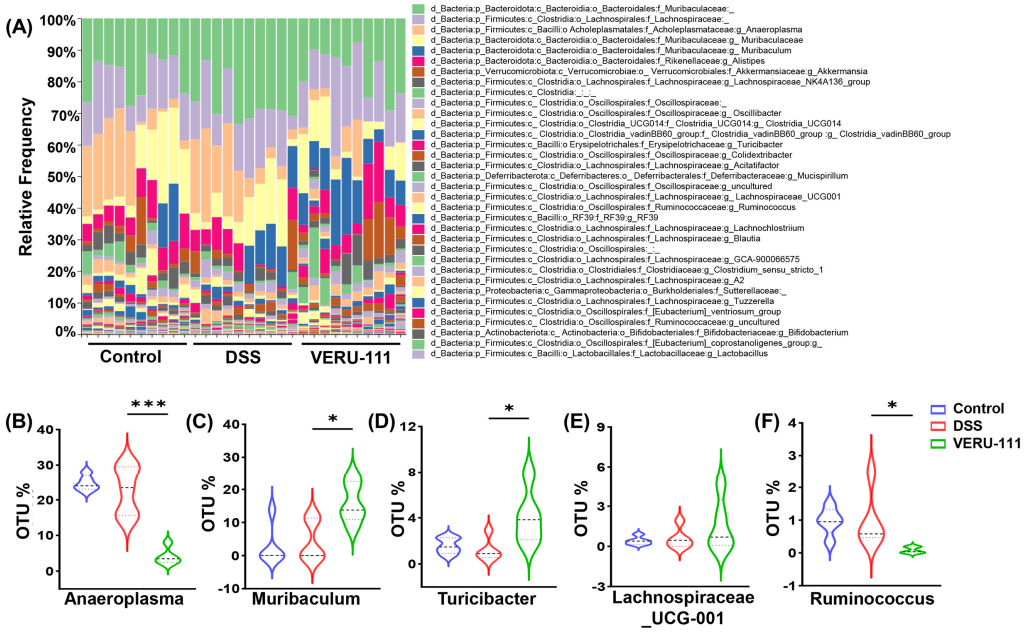

Figure 5. VERU-111 restored the abundance of commensal gut genera that was altered by administration of DSS. (A) Taxonomic composition analysis showing the relative abundance of the major bacterial genera in fecal samples from three experimental groups. (**B–F**) The relative abundance of key genera that were significantly altered by VERU-111 treatment. Violin plots depict the distribution of OTU percentage for **(B)** *Anaeroplasma*, **(C)** *Muribaculum*, **(D)** *Turicibacter*, **(E)** *Lachnospiraceae UCG-001*, and **(F)** *Ruminococcus*. Violin plots represent mean values ± SEM. Statistical analysis was performed using one-way ANOVA followed by Student's t-test. (* $p < 0.05$, *** $p < 0.001$).

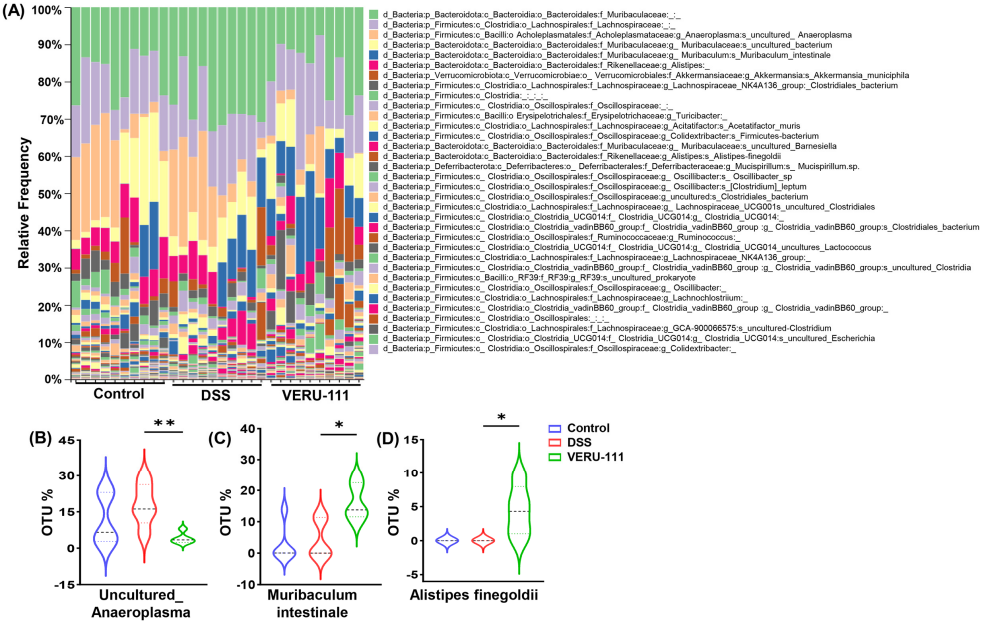

 doi:10.20944/preprints202512.1903.v1

Figure 6. Treatment with VERU-111 restores specific healthy gut microbial species altered by DSS. (A) Taxonomic composition analysis showing the relative abundance of the most prevalent bacterial species in fecal samples from three groups of experimental mice. Violin plots depict the distribution of OTU percentage for **(B)** *Uncultured Anaeroplasma*, **(C)** *Muribaculum intestinale*, and **(D)** *Alistipes finegoldii*. Violin plots represent mean ± SEM. Statistical analysis was performed using one-way ANOVA followed by Student's t-test. (* $p < 0.05$, ** $p < 0.01$).

3.5. Prediction of Functional Capacity of Microbiome Through KEGG Pathway Analysis

We used Kyoto Encyclopedia of Genes and Genomes (KEGG) pathway analysis to generate heatmaps that illustrate the potential functional capacity of GM communities that were altered after VERU-111 treatment. In the DSS-induced CRC, GM functional pathways were markedly dysregulated, with elevated activity in disease-related pathways, cellular metabolic processes, and environmental information processing pathways. Treatment with VERU-111 substantially normalized these functional alterations, particularly in metabolism and genetic information processing pathways (**Figure 7A**). Further analysis within each major shift revealed that metabolic function, including amino acid, lipid, carbohydrate, terpenoid, and polyketide metabolism, was upregulated in the mice with DSS-induced CRC. In contrast, treatment of these mice with VERU-111 normalized that pattern toward that observed in naïve mice. Moreover, DSS-challenged mice exhibited a pronounced increment of pathways related to membrane transporters and human disease-related modules, which were reversed through VERU-111 treatment (**Figure 7B**).

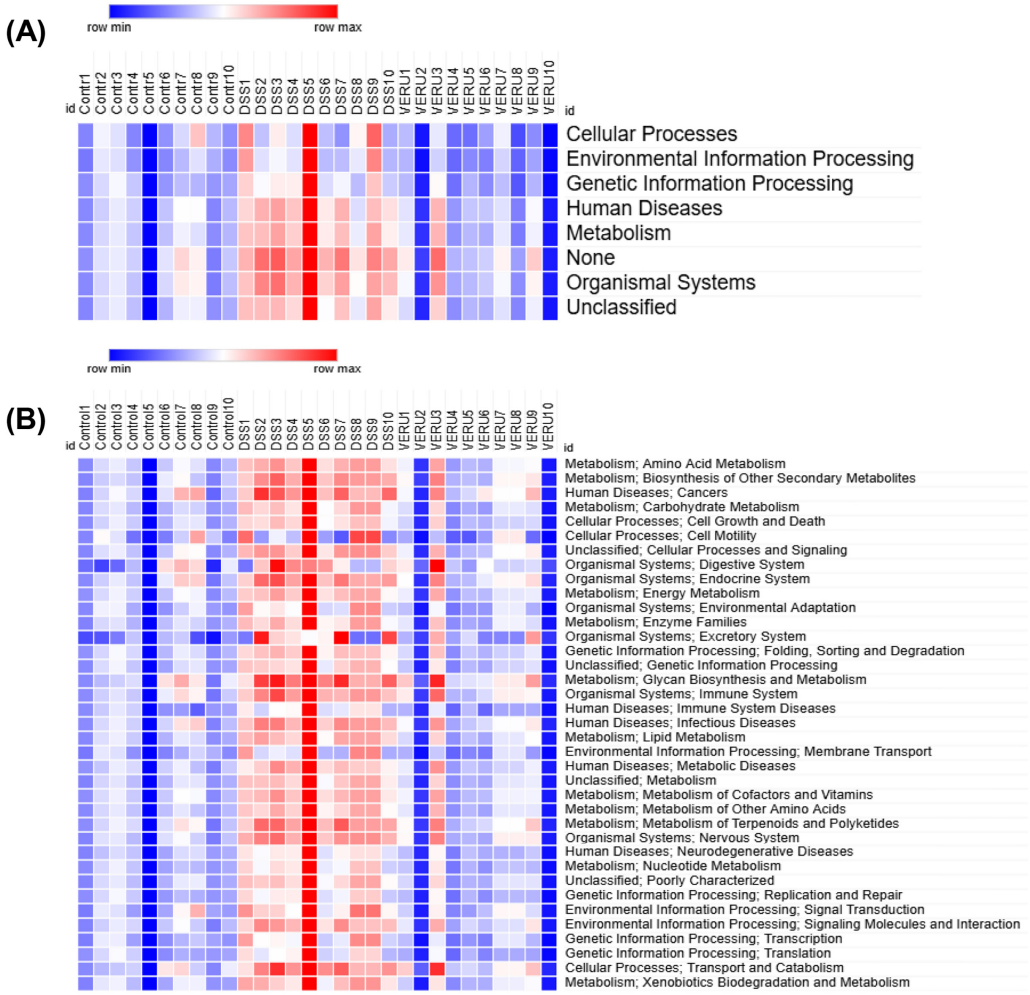

 doi:10.20944/preprints202512.1903.v1

Figure 7. Predicted key functional profiles of gut microbiota altered by VERU-111 treatment. Heatmap analysis of KEGG functional pathways predicted from 16S rRNA gene sequencing data. **(A)** Heatmap shows clustering of broad functional categories (Level 1) across Control, DSS, and VERU-111 treated groups. **(B)** Detailed heatmap shows specific metabolic and cellular pathways (Level 2). The color scale represents the relative abundance of each functional category in each sample, ranging from blue (row minimum) to red (row maximum). Overall, the DSS group exhibited a distinct functional profile compared to the Control group, while VERU-111 treatment shifted the profile toward the Control phenotype.

At level 3 KEGG pathway analysis for specific metabolic processes, we observed significant upregulation of several metabolic pathways, including biotin, glycolipid, and lipoic acid metabolism, biosynthesis of folate and the aromatic amino acids phenylalanine, tyrosine, and tryptophan, and degradation of xylene in DSS-challenged mice relative to naïve mice. Notably, in mice treated with VERU-111, these pathways were restored to normal homeostatic levels (**Figure 8A-C**). Together, these findings suggest that VERU-111 elicits a corrective effect on microbiome functional dysregulation that contributes to the restoration of gut microbial homeostasis.

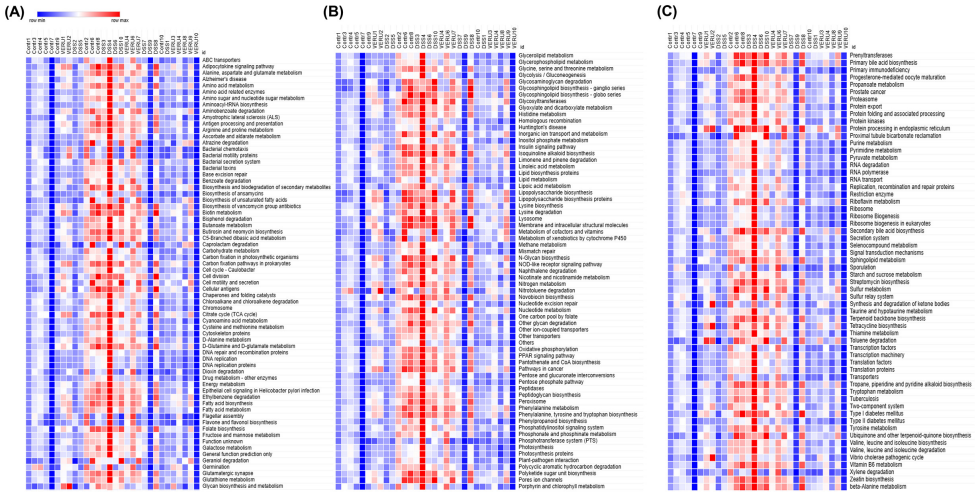

Figure 8. Detailed heatmap of KEGG Level 3 pathways showed a homeostatic restoration of key metabolic pathways in mice treated with VERU-111. (A-C) KEGG Level 3 functional pathways across all samples (Control, DSS, and VERU-111 groups). Color intensity represents the relative abundance of each pathway (Red = high abundance, Blue = low abundance). This visualization delves into in-depth information on the functional shifts induced by DSS and their subsequent restoration by VERU-111 treatment.

4. Discussion

Rich microbial diversity and high population levels are hallmarks of a healthy gut microbiome (GM), while this diversity becomes highly dysregulated when a mammalian host experiences one of many pathological conditions, including CRC [42,43]. In this study, we used the experimental animal model of CRC to show that mice treated with VERU-111 demonstrated a marked healthy shift that reversed the dysbiosis caused by DSS. Mice receiving DSS + VERU-111 showed an increased microbial diversity and enrichment of beneficial taxa, alongside a reduction of potentially disease-friendly taxa. Such a shift in microbial diversity is consistent with an improved immune-responsive gut microbial ecosystem and improved responsiveness to chemotherapy or immune checkpoint blockade (ICB) therapy like anti-PD-1. VERU-111 treatment normalized several DSS-induced metabolic pathway dysregulations, including those affecting lipid metabolism and folate biosynthesis. A major protective mechanism exerted by a healthy GM is the production of short-chain fatty acids, including butyrate, which is associated with disease-free survival [44]. Higher bacterial diversity, including commensal bacterial richness, is strongly associated with higher disease-free

 doi:10.20944/preprints202512.1903.v1

survival with CRC [45]. In this study, DSS-challenged mice exhibited an induction of dysbiosis and fecal samples with lower bacterial abundance, while treatment with VERU-111 reversed the dysbiosis and improved both alpha and beta diversity. *Akkermansia muciniphila* bacteria have a symbiotic effect that accelerates the production of butyrate by butyrogenic bacterial taxa [46]. Interestingly, we found a notable increase in the *Akkermansiaceae* and the *Rikenellaceae* families on treatment with VERU-111. The class *Clostridia* species *Blautia wexlerae* exerts a similar symbiotic effect that assists other GM species to produce propionate and butyrate, which are excreted in the feces [47]. Relative to mice treated with DSS alone, mice treated with VERU-111 exhibited an increased abundance of *Clostridia* and of *Muribaculum intestinale.* In a mouse model of cancer cachexia, *Muribaculum intestinale* is significantly depleted in the GM, leading to a disease condition characterized by diminished butyrate production that improved on supplementation with *Muribaculum intestinale* [40]. Taken together, these data indicate that VERU-111 treatment restructured the gut microbiome by increasing bacterial diversity and promoting the expansion of butyrate-producing taxa, changes that are likely to contribute to its tumor-suppressive effects.

During cancer, GM profiles can serve as predictive biomarkers of treatment efficacy and prognosis [10]. The crosstalk between the GM and chemotherapy could significantly advance our understanding of cancer therapy and patient outcomes, but this area of research is still limited. Chemotherapy induces GM dysbiosis and perturbs the integrity of the gastrointestinal mucosal barrier, thereby accelerating mucosal inflammation and resulting in chemotherapy-induced gastrointestinal mucositis [48]. A clinical study shows that GM alterations in 94 patients who received a standard 5–Fluorouracil–based adjuvant chemotherapy following radical surgery for advanced CRC reported an increased abundance of *Fusobacterium nucleatum,* which is related to negative outcomes in CRC [49]. Bacteria from the phylum *Proteobacteria* can metabolize the chemotherapeutic drug gemcitabine into its inactive form (2′,2′-difluorodeoxyuridine) [12]. In the present study, we did not detect any major changes in the *Fusobacteria* or *Proteobacteria* phyla. The family *Akkermansiaceae* species *Akkermansia muciniphila* boosts the effectiveness of many chemotherapeutics like FOLFOX (oxaliplatin, fluorouracil, and calcium folinate) in CRC patients [50]. A combination of tyrosine kinase inhibitors and ICB therapy potentiates the immunotherapy response by increasing the growth of *Muribaculum* and its metabolite, urocanic acid, which ultimately reduces the recruitment of myeloid-derived suppressor cells (MDSCs) via the CXCL1-CXCR2 axis [51]. Our findings of higher abundance of *Akkermansiaceae* and *Muribaculum* in fecal samples from mice in the VERU-111-treated group than those treated with DSS alone corroborate these earlier findings.

The efficacy of immunotherapy is strongly affected by the GM, which modulates host immune responses and participates in the remodeling of the tumor microenvironment [52]. In preclinical studies, mice harboring a favorable GM exhibit significantly enhanced responses to anti–PD-L1 therapy than those carrying an unfavorable GM. This advantage can be conferred exogenously via cohousing or fecal transplant [53]. The loss of GM diversity is associated with poor treatment outcomes of ICB therapy, whereas enrichment of bacterial flora, including *Faecalibacterium*, *Bifidobacterium*, *Lactobacillus*, and *Akkermansia muciniphila,* has a favorable impact on ICB therapy [53–56]. Further, another study reported a higher abundance of bacteria in the genus *Turicibacter* in a patient who was responsive to anti-PD-1 therapy, relative to that in the non-responsive patient cohort [57]. In our study, mice subjected to VERU-111 treatment exhibited a favorable GM diversity characterized by improved abundance of healthy bacteria, including members of the family *Akkermansiaceae* and the genus *Turicibacter* (phylum *Bacillota,* formerly known as *Firmicutes*). In a clinical trial, patients with anti-PD-1-refractory melanoma who received a fecal microbiota transplant from a patient who responded to anti-PD-1 therapy demonstrated a better response, increased activation of $CD8^+$ T cells, and suppression of interleukin-8–expressing myeloid cells [58]. Together, these previous preclinical and clinical studies highlight the role of GM in shaping the response to ICB therapy, with distinct effects being observed with different bacterial taxa. Our study depicted the richness of ICB therapy-favorable taxa in mice treated with VERU-111 with DSS relative to those treated with DSS alone. Future mechanistic studies are required, which may incorporate a paradigm

 doi:10.20944/preprints202512.1903.v1

shift that targets the modulation of the gut microbiota to optimize immunotherapy response in CRC patients and perhaps all cancer patients.

The response of patients to cancer therapy varies substantially from person to person and is closely associated with host immune status [59–61]. Importantly, growing evidence confirms the influence of GM on tumor immunity [62]. Beneficial commensal microbes augment both innate and adaptive immunity, while cancer-associated dysbiosis can dampen the host immune response [63]. The GM plays a crucial role in shaping patients' responses to cancer therapies via interactions with diverse immune cell populations [64]. For example, GM-derived metabolites and altered metabolic pathways play a crucial role in regulating immune cells, including T cells, B cells, dendritic cells, and macrophages [65]. Short-chain fatty acids produced by organisms in the GM augment $CD8^+$ T cell effector functions by modifying their cellular metabolism [66]. In this study, KEGG pathway analysis of the 16S RNA sequencing data from samples in the different experimental groups depicted a dysregulation in metabolism and human disease-related pathways in response to DSS insult. In mice treated with DSS alone, metabolism of amino acids, lipids, carbohydrates, terpenoids, and polyketides was upregulated. This is not surprising since lipid metabolism is frequently upregulated in cancer to support high-energy demands and the rapid growth of tumor cells, allowing the tumor cells to proliferate and resist apoptosis [67,68]. Folic acid plays an important role in cellular regulation, and during CRC, the folate metabolic pathway is upregulated to facilitate the rapid growth of tumor cells [69]. Data from our KEGG pathway analysis of DSS-treated mice corroborates a similar pattern of upregulated biosynthesis of folate and aromatic amino acids, metabolism of biotin and lipoic acid, and degradation of xylene. Interestingly, treatment of mice with DSS and VERU-111 restored these pathways to more normal levels. Thus, by suppressing these metabolic pathways, VERU-111 may reinforce its intended therapeutic effect of lowering tumor burden. Taken together, our data indicate that VERU-111 treatment restores the DSS-induced dysregulation of metabolic pathways and perturbs key pathways that supply energy to tumor cells, thereby promoting their death and suppressing tumorigenesis.

5. Conclusions

In summary, in an experimental murine model of CRC, VERU-111 improved both alpha and beta diversity of the GM diversity, characterized by an increased proportion of healthy bacterial taxa. These alterations of the microbiome and the restoration of dysregulated metabolic pathways by VERU-111 are novel and depict the safety of this drug candidate. These data also indicate that VERU-111 may enhance the efficacy of conventional chemotherapy and immunotherapy for the treatment of CRC. Moreover, our study outcomes provide a rationale for the development of future therapeutic approaches that integrate microbiome-targeted intervention with standard CRC therapy, potentially improving treatment outcomes.

Author Contributions: Md Abdullah Al Mamun: Performed most of the animal experiments, data curation, and data analysis, wrote the first draft of the manuscript. Ahmed Rakib: Participated in the experiments and made the figures. Mousumi Mandal: Participated in the experiments, reviewed, and edited the manuscript. Duane D. Miller, Dong-Hao Chen, and Wei Li: Conceived the idea of VERU-111, synthesized the compound, and edited the manuscript. Mitzi Nagarkatti and Prakash Nagarkatti performed 16S rRNA Amplicon Sequencing and data analysis. Udai P. Singh: Conceived the idea, reviewed, and edited the manuscript.

Funding: This study was supported by grants from the National Institutes of Health (NIH) (NIAID R01 AI140405) to the U.S. at UTHSC in Memphis, TN.

Institutional Review Board Statement: All animal experimentation was performed under a protocol (number UPS 23-0450) approved by the Institutional Animal Care and Use Committee (IACUC) at our institution. All animal handling and experimental procedures involving animals were performed to minimize pain and discomfort. The study design and analysis were conducted with the utmost consideration for reducing animal suffering and minimizing the number of animals used. All personnel involved in the animal studies were trained

 doi:10.20944/preprints202512.1903.v1

in animal care and handling to ensure that the highest standards of animal welfare and ethical conduct were maintained throughout the research.

Informed Consent Statement: No patient samples were used during the course of our analysis, so informed consent was not required.

Data Availability Statement: The raw data described in this manuscript will be made available to the public by the authors, without any reservation.

Conflicts of Interest: The authors declare that they have no competing interests that could influence this study and have not been involved with any study sponsors.

References

1. Cahenzli, J.; Köller, Y.; Wyss, M.; Geuking, M.B.; McCoy, K.D. Intestinal microbial diversity during early-life colonization shapes long-term IgE levels. *Cell host & microbe* **2013**, *14*, 559-570.
2. Zhao, L.-Y.; Mei, J.-X.; Yu, G.; Lei, L.; Zhang, W.-H.; Liu, K.; Chen, X.-L.; Kołat, D.; Yang, K.; Hu, J.-K. Role of the gut microbiota in anticancer therapy: from molecular mechanisms to clinical applications. *Signal Transduction and Targeted Therapy* **2023**, *8*, 201.
3. Zheng, D.; Liwinski, T.; Elinav, E. Interaction between microbiota and immunity in health and disease. *Cell research* **2020**, *30*, 492-506.
4. Sadrekarimi, H.; Gardanova, Z.R.; Bakhshesh, M.; Ebrahimzadeh, F.; Yaseri, A.F.; Thangavelu, L.; Hasanpoor, Z.; Zadeh, F.A.; Kahrizi, M.S. Emerging role of human microbiome in cancer development and response to therapy: special focus on intestinal microflora. *Journal of translational medicine* **2022**, *20*, 301.
5. Zhao, K.; Hu, Y. Microbiome harbored within tumors: a new chance to revisit our understanding of cancer pathogenesis and treatment. *Signal Transduction and Targeted Therapy* **2020**, *5*, 136.
6. Wong-Rolle, A.; Wei, H.; Zhao, C.; Jin, C. Unexpected guests in the tumor microenvironment: microbiome in cancer. Protein Cell 12: 426–435. **2021**.
7. Wong, C.C.; Yu, J. Gut microbiota in colorectal cancer development and therapy. *Nature Reviews Clinical Oncology* **2023**, *20*, 429-452.
8. Carding, S.; Verbeke, K.; Vipond, D.T.; Corfe, B.M.; Owen, L.J. Dysbiosis of the gut microbiota in disease. *Microbial ecology in health and disease* **2015**, *26*, 26191.
9. Rebersek, M. Gut microbiome and its role in colorectal cancer. *BMC cancer* **2021**, *21*, 1325.
10. Kim, J.; Lee, H.K. Potential role of the gut microbiome in colorectal cancer progression. *Frontiers in immunology* **2022**, *12*, 807648.
11. Iida, N.; Dzutsev, A.; Stewart, C.A.; Smith, L.; Bouladoux, N.; Weingarten, R.A.; Molina, D.A.; Salcedo, R.; Back, T.; Cramer, S. Commensal bacteria control cancer response to therapy by modulating the tumor microenvironment. *science* **2013**, *342*, 967-970.
12. Geller, L.T.; Barzily-Rokni, M.; Danino, T.; Jonas, O.H.; Shental, N.; Nejman, D.; Gavert, N.; Zwang, Y.; Cooper, Z.A.; Shee, K. Potential role of intratumor bacteria in mediating tumor resistance to the chemotherapeutic drug gemcitabine. *Science* **2017**, *357*, 1156-1160.
13. Flanagan, L.; Schmid, J.; Ebert, M.; Soucek, P.; Kunicka, T.; Liska, V.; Bruha, J.; Neary, P.; Dezeeuw, N.; Tommasino, M. Fusobacterium nucleatum associates with stages of colorectal neoplasia development, colorectal cancer and disease outcome. *European journal of clinical microbiology & infectious diseases* **2014**, *33*, 1381-1390.
14. Mima, K.; Nishihara, R.; Qian, Z.R.; Cao, Y.; Sukawa, Y.; Nowak, J.A.; Yang, J.; Dou, R.; Masugi, Y.; Song, M. Fusobacterium nucleatum in colorectal carcinoma tissue and patient prognosis. *Gut* **2016**, *65*, 1973-1980.
15. Mahmoudian, F.; Gheshlagh, S.R.; Hemati, M.; Farhadi, S.; Eslami, M. The influence of microbiota on the efficacy and toxicity of immunotherapy in cancer treatment. *Molecular Biology Reports* **2025**, *52*, 86.
16. Said, S.S.; Ibrahim, W.N. Breaking barriers: the promise and challenges of immune checkpoint inhibitors in triple-negative breast cancer. *Biomedicines* **2024**, *12*, 369.
17. Spencer, C.N.; McQuade, J.L.; Gopalakrishnan, V.; McCulloch, J.A.; Vetizou, M.; Cogdill, A.P.; Khan, M.A.W.; Zhang, X.; White, M.G.; Peterson, C.B. Dietary fiber and probiotics influence the gut microbiome and melanoma immunotherapy response. *Science* **2021**, *374*, 1632-1640.

 doi:10.20944/preprints202512.1903.v1

18. Yang, Y. Cancer immunotherapy: harnessing the immune system to battle cancer. *The Journal of clinical investigation* **2015**, *125*, 3335-3337.
19. André, T.; Shiu, K.-K.; Kim, T.W.; Jensen, B.V.; Jensen, L.H.; Punt, C.; Smith, D.; Garcia-Carbonero, R.; Benavides, M.; Gibbs, P. Pembrolizumab in microsatellite-instability–high advanced colorectal cancer. *New England Journal of Medicine* **2020**, *383*, 2207-2218.
20. Chung, Y.; Ryu, Y.; An, B.C.; Yoon, Y.-S.; Choi, O.; Kim, T.Y.; Yoon, J.; Ahn, J.Y.; Park, H.J.; Kwon, S.-K. A synthetic probiotic engineered for colorectal cancer therapy modulates gut microbiota. *Microbiome* **2021**, *9*, 122.
21. Cheng, W.; Li, F.; Yang, R. The roles of gut microbiota metabolites in the occurrence and development of colorectal cancer: Multiple insights for potential clinical applications. *Gastro Hep Advances* **2024**, *3*, 855-870.
22. Luo, W.; Li, R.; Pan, C.; Luo, C. Gut microbiota–derived metabolites in immunomodulation and gastrointestinal cancer immunotherapy. *Frontiers in Immunology* **2025**, *16*, 1710880.
23. Wang, Q.; Arnst, K.E.; Wang, Y.; Kumar, G.; Ma, D.; Chen, H.; Wu, Z.; Yang, J.; White, S.W.; Miller, D.D. Structural modification of the 3, 4, 5-trimethoxyphenyl moiety in the tubulin inhibitor VERU-111 leads to improved antiproliferative activities. *Journal of medicinal chemistry* **2018**, *61*, 7877-7891.
24. Kashyap, V.K.; Dan, N.; Chauhan, N.; Wang, Q.; Setua, S.; Nagesh, P.K.; Malik, S.; Batra, V.; Yallapu, M.M.; Miller, D.D. VERU-111 suppresses tumor growth and metastatic phenotypes of cervical cancer cells through the activation of p53 signaling pathway. *Cancer letters* **2020**, *470*, 64-74.
25. Deng, S.; Krutilina, R.I.; Wang, Q.; Lin, Z.; Parke, D.N.; Playa, H.C.; Chen, H.; Miller, D.D.; Seagroves, T.N.; Li, W. An orally available tubulin inhibitor, VERU-111, suppresses triple-negative breast cancer tumor growth and metastasis and bypasses taxane resistance. *Molecular cancer therapeutics* **2020**, *19*, 348-363.
26. Mahmud, F.; Deng, S.; Chen, H.; Miller, D.D.; Li, W. Orally available tubulin inhibitor VERU-111 enhances antitumor efficacy in paclitaxel-resistant lung cancer. *Cancer letters* **2020**, *495*, 76-88.
27. Krutilina, R.I.; Hartman, K.L.; Oluwalana, D.; Playa, H.C.; Parke, D.N.; Chen, H.; Miller, D.D.; Li, W.; Seagroves, T.N. Sabizabulin, a potent orally bioavailable colchicine binding site agent, suppresses HER2+ breast cancer and metastasis. *Cancers* **2022**, *14*, 5336.
28. Busbee, P.B.; Menzel, L.; Alrafas, H.R.; Dopkins, N.; Becker, W.; Miranda, K.; Tang, C.; Chatterjee, S.; Singh, U.P.; Nagarkatti, M. Indole-3-carbinol prevents colitis and associated microbial dysbiosis in an IL-22–dependent manner. *JCI insight* **2020**, *5*.
29. Nagalingam, N.A.; Kao, J.Y.; Young, V.B. Microbial ecology of the murine gut associated with the development of dextran sodium sulfate-induced colitis. *Inflammatory bowel diseases* **2011**, *17*, 917-926.
30. Segata, N.; Izard, J.; Waldron, L.; Gevers, D.; Miropolsky, L.; Garrett, W.S.; Huttenhower, C. Metagenomic biomarker discovery and explanation. *Genome biology* **2011**, *12*, R60.
31. Yachida, S.; Mizutani, S.; Shiroma, H.; Shiba, S.; Nakajima, T.; Sakamoto, T.; Watanabe, H.; Masuda, K.; Nishimoto, Y.; Kubo, M. Metagenomic and metabolomic analyses reveal distinct stage-specific phenotypes of the gut microbiota in colorectal cancer. *Nature medicine* **2019**, *25*, 968-976.
32. Thomas, A.M.; Jesus, E.C.; Lopes, A.; Aguiar Jr, S.; Begnami, M.D.; Rocha, R.M.; Carpinetti, P.A.; Camargo, A.A.; Hoffmann, C.; Freitas, H.C. Tissue-associated bacterial alterations in rectal carcinoma patients revealed by 16S rRNA community profiling. *Frontiers in cellular and infection microbiology* **2016**, *6*, 179.
33. Pongen, Y.L.; Thirumurugan, D.; Ramasubburayan, R.; Prakash, S. Harnessing actinobacteria potential for cancer prevention and treatment. *Microbial Pathogenesis* **2023**, *183*, 106324.
34. Lee, N.-K.; Kim, W.-S.; Paik, H.-D. Bacillus strains as human probiotics: characterization, safety, microbiome, and probiotic carrier. *Food science and biotechnology* **2019**, *28*, 1297-1305.
35. Huycke, M.M.; Abrams, V.; Moore, D.R. Enterococcus faecalis produces extracellular superoxide and hydrogen peroxide that damages colonic epithelial cell DNA. *Carcinogenesis* **2002**, *23*, 529-536.
36. Gubernatorova, E.O.; Gorshkova, E.A.; Bondareva, M.A.; Podosokorskaya, O.A.; Sheynova, A.D.; Yakovleva, A.S.; Bonch-Osmolovskaya, E.A.; Nedospasov, S.A.; Kruglov, A.A.; Drutskaya, M.S. Akkermansia muciniphila-friend or foe in colorectal cancer? *Frontiers in immunology* **2023**, *14*, 1303795.
37. Liu, N.; Zou, S.; Xie, C.; Meng, Y.; Xu, X. Effect of the β-glucan from Lentinus edodes on colitis-associated colorectal cancer and gut microbiota. *Carbohydrate Polymers* **2023**, *316*, 121069.

 doi:10.20944/preprints202512.1903.v1

38. Lin, T.-C.; Soorneedi, A.; Guan, Y.; Tang, Y.; Shi, E.; Moore, M.D.; Liu, Z. Turicibacter fermentation enhances the inhibitory effects of Antrodia camphorata supplementation on tumorigenic serotonin and Wnt pathways and promotes ROS-mediated apoptosis of Caco-2 cells. *Frontiers in pharmacology* **2023**, *14*, 1203087.
39. Gates, T.J.; Yuan, C.; Shetty, M.; Kaiser, T.; Nelson, A.C.; Chauhan, A.; Starr, T.K.; Staley, C.; Subramanian, S. Fecal microbiota restoration modulates the microbiome in inflammation-driven colorectal cancer. *Cancers* **2023**, *15*, 2260.
40. Li, L.; Lian, P.; Dong, W.; Song, S.; Wazir, J.; Wang, R.; Lin, K.; Pu, W.; Lu, R.; Yu, Z. Restoring Muribaculum intestinale–Derived Butyrate Mitigates Skeletal Muscle Loss in Cancer Cachexia. *Journal of Cachexia, Sarcopenia and Muscle* **2025**, *16*, e70140.
41. Wu, Z.-Y.; Wu, Q.-W.; Han, Y.; Xiang, S.-J.; Wang, Y.-N.; Wu, W.-W.; Chen, Y.-X.; Feng, Z.-Q.; Wang, Y.-Y.; Xu, Z.-G. Alistipes finegoldii augments the efficacy of immunotherapy against solid tumors. *Cancer Cell* **2025**, *43*, 1714-1730. e1712.
42. Van Hul, M.; Cani, P.D.; Petitfils, C.; De Vos, W.M.; Tilg, H.; El-Omar, E.M. What defines a healthy gut microbiome? *Gut* **2024**, *73*, 1893-1908.
43. Zhao, L.; Cho, W.C.; Nicolls, M.R. Colorectal cancer-associated microbiome patterns and signatures. *Frontiers in Genetics* **2021**, *12*, 787176.
44. Kaźmierczak-Siedlecka, K.; Marano, L.; Merola, E.; Roviello, F.; Połom, K. Sodium butyrate in both prevention and supportive treatment of colorectal cancer. *Frontiers in Cellular and Infection Microbiology* **2022**, *12*, 1023806.
45. Byrd, D.A.; Damerell, V.; Gomez Morales, M.F.; Hogue, S.R.; Lin, T.; Ose, J.; Himbert, C.; Ilozumba, M.N.; Kahlert, C.; Shibata, D. The gut microbiome is associated with disease-free survival in stage I–III colorectal cancer patients. *International Journal of Cancer* **2025**, *157*, 64-73.
46. Belzer, C.; Chia, L.W.; Aalvink, S.; Chamlagain, B.; Piironen, V.; Knol, J.; de Vos, W.M. Microbial metabolic networks at the mucus layer lead to diet-independent butyrate and vitamin B12 production by intestinal symbionts. *MBio* **2017**, *8*, 10.1128/mbio. 00770-00717.
47. Hosomi, K.; Saito, M.; Park, J.; Murakami, H.; Shibata, N.; Ando, M.; Nagatake, T.; Konishi, K.; Ohno, H.; Tanisawa, K. Oral administration of Blautia wexlerae ameliorates obesity and type 2 diabetes via metabolic remodeling of the gut microbiota. *Nature communications* **2022**, *13*, 4477.
48. Yixia, Y.; Sripetchwandee, J.; Chattipakorn, N.; Chattipakorn, S.C. The alterations of microbiota and pathological conditions in the gut of patients with colorectal cancer undergoing chemotherapy. *Anaerobe* **2021**, *68*, 102361.
49. Zhang, S.; Yang, Y.; Weng, W.; Guo, B.; Cai, G.; Ma, Y.; Cai, S. Fusobacterium nucleatum promotes chemoresistance to 5-fluorouracil by upregulation of BIRC3 expression in colorectal cancer. *Journal of Experimental & Clinical Cancer Research* **2019**, *38*, 14.
50. Hou, X.; Zhang, P.; Du, H.; Chu, W.; Sun, R.; Qin, S.; Tian, Y.; Zhang, Z.; Xu, F. Akkermansia muciniphila potentiates the antitumor efficacy of FOLFOX in colon cancer. *Frontiers in Pharmacology* **2021**, *12*, 725583.
51. Zhang, M.; Wei, Z.; Wei, B.; Lai, C.; Zong, G.; Tao, E.; Fan, M.; Pan, Y.; Zhou, B.; Shen, L. Microbiota-derived urocanic acid triggered by tyrosine kinase inhibitors potentiates cancer immunotherapy efficacy. *Cell Host & Microbe* **2025**, *33*, 915-931. e919.
52. Lei, W.; Zhou, K.; Lei, Y.; Li, Q.; Zhu, H. Gut microbiota shapes cancer immunotherapy responses. *npj Biofilms and Microbiomes* **2025**, *11*, 143.
53. Sivan, A.; Corrales, L.; Hubert, N.; Williams, J.B.; Aquino-Michaels, K.; Earley, Z.M.; Benyamin, F.W.; Man Lei, Y.; Jabri, B.; Alegre, M.-L. Commensal Bifidobacterium promotes antitumor immunity and facilitates anti–PD-L1 efficacy. *Science* **2015**, *350*, 1084-1089.
54. Gopalakrishnan, V.; Spencer, C.N.; Nezi, L.; Reuben, A.; Andrews, M.C.; Karpinets, T.V.; Prieto, P.; Vicente, D.; Hoffman, K.; Wei, S.C. Gut microbiome modulates response to anti–PD-1 immunotherapy in melanoma patients. *Science* **2018**, *359*, 97-103.
55. Chaput, N.; Lepage, P.; Coutzac, C.; Soularue, E.; Le Roux, K.; Monot, C.; Boselli, L.; Routier, E.; Cassard, L.; Collins, M. Baseline gut microbiota predicts clinical response and colitis in metastatic melanoma patients treated with ipilimumab. *Annals of Oncology* **2017**, *28*, 1368-1379.

 doi:10.20944/preprints202512.1903.v1

56. Zheng, Y.; Wang, T.; Tu, X.; Huang, Y.; Zhang, H.; Tan, D.; Jiang, W.; Cai, S.; Zhao, P.; Song, R. Gut microbiome affects the response to anti-PD-1 immunotherapy in patients with hepatocellular carcinoma. *Journal for immunotherapy of cancer* **2019**, *7*, 193.
57. Hamada, K.; Isobe, J.; Hattori, K.; Hosonuma, M.; Baba, Y.; Murayama, M.; Narikawa, Y.; Toyoda, H.; Funayama, E.; Tajima, K. Turicibacter and Acidaminococcus predict immune-related adverse events and efficacy of immune checkpoint inhibitor. *Frontiers in immunology* **2023**, *14*, 1164724.
58. Davar, D.; Dzutsev, A.K.; McCulloch, J.A.; Rodrigues, R.R.; Chauvin, J.-M.; Morrison, R.M.; Deblasio, R.N.; Menna, C.; Ding, Q.; Pagliano, O. Fecal microbiota transplant overcomes resistance to anti–PD-1 therapy in melanoma patients. *Science* **2021**, *371*, 595-602.
59. Chen, Y.; Jia, K.; Sun, Y.; Zhang, C.; Li, Y.; Zhang, L.; Chen, Z.; Zhang, J.; Hu, Y.; Yuan, J. Predicting response to immunotherapy in gastric cancer via multi-dimensional analyses of the tumour immune microenvironment. *Nature communications* **2022**, *13*, 4851.
60. Fridman, W.H.; Pagès, F.; Sautès-Fridman, C.; Galon, J. The immune contexture in human tumours: impact on clinical outcome. *Nature Reviews Cancer* **2012**, *12*, 298-306.
61. Spranger, S.; Sivan, A.; Corrales, L.; Gajewski, T.F. Tumor and host factors controlling antitumor immunity and efficacy of cancer immunotherapy. *Advances in immunology* **2016**, *130*, 75-93.
62. Cremonesi, E.; Governa, V.; Garzon, J.F.G.; Mele, V.; Amicarella, F.; Muraro, M.G.; Trella, E.; Galati-Fournier, V.; Oertli, D.; Däster, S.R. Gut microbiota modulate T cell trafficking into human colorectal cancer. *Gut* **2018**, *67*, 1984-1994.
63. Ibrahim, A.; Hugerth, L.W.; Hases, L.; Saxena, A.; Seifert, M.; Thomas, Q.; Gustafsson, J.Å.; Engstrand, L.; Williams, C. Colitis-induced colorectal cancer and intestinal epithelial estrogen receptor beta impact gut microbiota diversity. *International journal of cancer* **2019**, *144*, 3086-3098.
64. Di Modica, M.; Gargari, G.; Regondi, V.; Bonizzi, A.; Arioli, S.; Belmonte, B.; De Cecco, L.; Fasano, E.; Bianchi, F.; Bertolotti, A. Gut microbiota condition the therapeutic efficacy of trastuzumab in HER2-positive breast cancer. *Cancer Research* **2021**, *81*, 2195-2206.
65. Yang, W.; Cong, Y. Gut microbiota-derived metabolites in the regulation of host immune responses and immune-related inflammatory diseases. *Cellular & molecular immunology* **2021**, *18*, 866-877.
66. Trompette, A.; Gollwitzer, E.S.; Pattaroni, C.; Lopez-Mejia, I.C.; Riva, E.; Pernot, J.; Ubags, N.; Fajas, L.; Nicod, L.P.; Marsland, B.J. Dietary fiber confers protection against flu by shaping Ly6c− patrolling monocyte hematopoiesis and CD8+ T cell metabolism. *Immunity* **2018**, *48*, 992-1005. e1008.
67. Vogel, F.C.; Chaves-Filho, A.B.; Schulze, A. Lipids as mediators of cancer progression and metastasis. *Nature cancer* **2024**, *5*, 16-29.
68. Wang, W.; Bai, L.; Li, W.; Cui, J. The lipid metabolic landscape of cancers and new therapeutic perspectives. *Frontiers in oncology* **2020**, *10*, 605154.
69. Zhu, Y.; Zhou, T.; Zheng, Y.; Yao, Y.; Lin, M.; Zeng, C.; Yan, Y.; Zhou, Y.; Li, D.-D.; Zhang, J. Folate metabolism-associated CYP26A1 is a clinico-immune target in colorectal cancer. *Genes & Immunity* **2025**, 1-18.